DOI 10.1007/s10946-018-9713-5
Journal of Russian Laser Research, Volume 39, Number 3, May, 2018

DAMPING IN THE INTERACTION OF A FIELD AND TWO THREE-LEVEL ATOMS THROUGH QUANTIZED CALDIROLA–KANAI HAMILTONIAN

Tarek M. El-Shahat,[1†] Mohamad Kh. Ismail,[1*] and Abdullah F. Al Naim[2]

[1] *Department of Mathematics, Faculty of Science*
Al-Azhar University, 71524, Assiut, Egypt

[2] *Physics Department, King Faisal University*
Alhasa-Hofuf, Saudi Arabia

[†]Corresponding author e-mail: el_shahat@yahoo.com
[*]Corresponding author e-mail: momran484@yahoo.com

Abstract

We investigate the damped interaction between two Λ-type three-level atoms and a quantized single-mode cavity field, for which the Hamiltonian of the field is rewritten in Caldirola–Kanai form. We obtain the wave functions for the case where the two atoms are initially prepared in arbitrary pure states and the field is initially prepared in the coherent state. We investigate numerically the influence of the damping parameter on the temporal behavior of the Mandel Q-parameter, linear entropy, and normal squeezing. We find the damping parameter and initial atomic states to play central roles in the nonclassical features and the degree of entanglement.

Keywords: three-level atom, linear entropy, Mandel parameter, normal squeezing, Caldirola–Kanai approach.

1. Introduction

The interaction model for a single quantized mode of a radiation field and a two-level atom in the rotating wave approximation (RWA) is called the Jaynes–Cummings model (JCM) [1]. This model has been the focus of many theoretical and experimental studies [2, 3]. The description of quantum friction in the classical formulation of quantum mechanics was considered in [4, 5]. Indeed, the main physical defect of the Caldirola–Kanai (CK) approach is that it implies the assumption that the quantum state of the system remains pure during its evolution, whereas the dissipation is always connected with the loss of quantum purity [6, 7]. Many different generalizations that modified the JCM using, for example, multimode fields [8], multilevel atoms [9–12], intensity-dependent (nonlinear regime) JCM [13, 14], and multiphoton transitions [15,16] have been proposed in recent decades. All of these studies have assumed an ideal system where damping is neglected; nevertheless, two Λ-type three-level atoms have been considered in [17, 18]. Entanglement plays a central role in the new field of quantum information, there being many studies concerning its properties [19]. The CK Hamiltonian has in this regard provided a vast area of research.

The problem of controlling entanglement using the quantized CK Hamiltonian has attracted much attention. This Hamiltonian was investigated in several quantum systems to study physical properties such

Manuscript submitted by the authors in English on May 18, 2018.

as plasma environments and mesoscopic (RLC) circuits [20,21]. The coherent states and squeezed states of the CK Hamiltonian were also studied [22,23] and showed that the eigenfunctions of the CK Hamiltonian satisfy the minimum uncertainty relation in a generalized form [24]. The many studies have examined different models in regard to the concept of damping [25, 26]. Caldirola and Kanai treated the problem of friction for a quantum harmonic oscillator by introducing a Hamiltonian with a time-dependent mass, called the CK Hamiltonian [27, 28],

$$H_{\rm CK} = \frac{\hat{p}^2}{2m_0}\exp(-2\gamma t) + \frac{1}{2}m_0\omega^2\hat{q}^2\exp(2\gamma t), \tag{1}$$

where ω, m_0, and γ are frequency, initial mass, and damping parameter, respectively. Furthermore, it is possible to introduce canonical transform [29] to reduce this Hamiltonian with its variable mass to a time-independent Hamiltonian in such a way that the uncertainty relation is preserved. Briefly, in this approach, the canonical transform introduced is $\hat{P} = e^{-\gamma t}\hat{p}$ and $\hat{Q} = e^{\gamma t}\hat{q}$ [30, 31] with the generating function $\Re_2(\hat{q}, \hat{P}, t) = e^{\gamma t}\dfrac{\hat{P}\hat{q} + \hat{q}\hat{P}}{2}$. As $\hat{p} = \dfrac{\partial\Re_2}{\partial\hat{q}}$ and $\hat{Q} = \dfrac{\partial\Re_2}{\partial\hat{P}}$, the transformed Hamiltonian is then $K = H_{\rm CK} + \dfrac{\partial\Re_2}{\partial t}$, which can be explicitly rewritten as

$$\hat{K} = \frac{\hat{P}^2}{2m_0} + \frac{1}{2}m_0\omega^2\hat{Q}^2 + \frac{\gamma}{2}(\hat{P}\hat{Q} + \hat{Q}\hat{P}). \tag{2}$$

The new momentum and position operators can then be written in terms of the usual creation and annihilation operators [30, 31],

$$\hat{P} = i\sqrt{\frac{\hbar m_0\omega}{2}}(\hat{a} + \hat{a}^\dagger), \qquad \hat{Q} = \sqrt{\frac{\hbar}{2m_0\omega}}(\hat{a}^\dagger - \hat{a}). \tag{3}$$

Next, the new ladder operators are defined as [32]

$$\begin{aligned} \hat{A} &= (2m_0\hbar\Omega)^{-1/2}[m_0(\Omega + i\gamma)\hat{Q} + i\hat{P}] = \tfrac{1}{2\sqrt{\Omega\omega}}(\zeta_+\hat{a} + \zeta_-\hat{a}^\dagger), \\ \hat{A}^\dagger &= (2m_0\hbar\Omega)^{-1/2}[m_0(\Omega - i\gamma)\hat{Q} - i\hat{P}] = \tfrac{1}{2\sqrt{\Omega\omega}}(\zeta_+^*\hat{a}^\dagger + \zeta_-^*\hat{a}), \end{aligned} \tag{4}$$

where $\Omega = \omega\sqrt{1-\eta^2}$, $\eta = \gamma/\omega$, and $\zeta_\pm = \Omega + i\gamma \pm \omega$. The relation $[\hat{A}, \hat{A}^\dagger] = 1$ is easily verified. Accordingly, the transformed Hamiltonian in terms of $\hat{A}$ and $\hat{A}^\dagger$ reads [32]

$$H_{\rm CK} = \hbar\Omega(\hat{A}^\dagger\hat{A} + 1/2). \tag{5}$$

However, as is seen, the Hamiltonian obtained is reduced from a variable mass Hamiltonian to a quantized Hamiltonian that does not explicitly depend on time. The system becomes a cavity containing a quantized multimode field that interacts with a multilevel atom, where the Hamiltonian of the quantized field is expressed according to the transformed Hamiltonian, i.e., the CK Hamiltonian, Eq. (5). The Hamiltonian of the whole system in the dipole approximation [33] is $H = H_{\rm free} + H_{\rm int}$, with

$$H_{\rm free} = \sum_k \Omega_k\hat{A}_k^\dagger\hat{A}_k + E_i\hat{\sigma}_{ii}, \qquad H_{\rm int} = \sum_{i,j}\sum_k \lambda_k^{ij}\hat{\sigma}_{ij}(\hat{A}_k^\dagger + \hat{A}_k), \tag{6}$$

where $\hat{\sigma}_{ij}$ represents the atomic operator $|i\rangle\langle j|$, and $|i\rangle$ denotes the atomic energy eigenstate with eigenvalue E_i, the factor 1/2 having been dropped. The subscript k is related to the kth mode of electromagnetic field, which is coupled to transition between atomic levels i, j by coupling constant $\lambda_k^{ij} = -\wp_{ij}\epsilon_k \pounds_k/\hbar$ [34]. Here $\pounds_k = e\langle i|\hat{r}|j\rangle$ is the electric-dipole transition matrix element also, and ϵ_k and $\pounds_k$ denote, respectively, the unit vector polarization vector and the amplitude of the kth mode of electric field. The interaction between a two-level atom with such a single-mode field, which is described by the CK Hamiltonian, has been studied in [33]. In [35], the interaction of such a damped field with a three-level atom having a Ξ-type configuration was examined, assuming that the quantized single-mode field undergoes dissipation described by the CK Hamiltonian. For any specific initial state with a given field intensity, the observed value for the maximum degree of entanglement (DEM) increases with increase in the value of the damping parameter.

In this paper, we investigate the interaction between two Λ-type three-level atoms and a single-mode quantized field with the CK Hamiltonian. After transforming the interaction Hamiltonian for the system, we obtain the probability amplitudes and the associated atom-field state vectors. In addition, we study the influence of the initial atomic states and damping parameters on the time behavior of the physical properties such as linear entropy, Mandel parameter, and normal squeezing.

The rest of this article is organized as follows.

In the next section, we derive the form of the probability amplitudes for the considered system. In Sec. 3, by considering different types of initial atomic states, we numerically investigate the effect of damping on the physical properties. Finally, in Sec. 4, we provide a summary.

2. Description of the Model

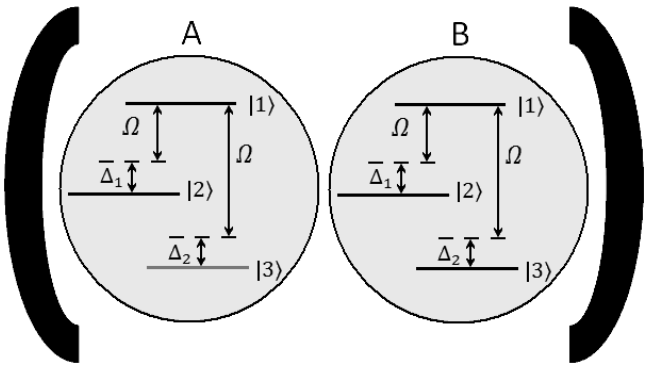

Fig. 1. Energy level diagram for two Λ-type three-level atoms coupled to a single-mode cavity field of frequency Ω with detunings Δ_1 and Δ_2.

The interaction between two Λ-type three-level atoms and a single-mode quantized field was investigated without damping in [17, 18]. In this work, we include damping of the quantized single-mode field, where it is described by the CK Hamiltonian. Here, the atomic levels are indicated by $|1\rangle$, $|2\rangle$, and $|3\rangle$ with energies $\omega_1 > \omega_2 > \omega_3$; transition $|2\rangle \leftrightarrow |3\rangle$ is forbidden in the electric-dipole approximation; the allowed transitions are $|1\rangle \leftrightarrow |2\rangle$ and $|1\rangle \leftrightarrow |3\rangle$; see Fig. 1. The free atomic and the field Hamiltonians are given by

$$H_0 = \sum_{j=A,B} (\omega_1 \hat{\sigma}_{11}^j + \omega_2 \hat{\sigma}_{22}^j + \omega_3 \hat{\sigma}_{33}^j) + \Omega \hat{A}^\dagger \hat{A}, \quad (7)$$

Accordingly, the atom–field Hamiltonian in the dipole approximation can be written as

$$H_{AB-f} = \sum_{j=A,B} \lambda_1^j (\hat{\sigma}_{12}^j + \hat{\sigma}_{21}^j)(\hat{A} + \hat{A}^\dagger) + \lambda_2^j (\hat{\sigma}_{13}^j + \hat{\sigma}_{31}^j)(\hat{A} + \hat{A}^\dagger), \quad (8)$$

where λ_1^j and λ_2^j are the atom-field coupling constants. The Hamiltonian H_{AB-f} in the interaction picture is

$$\begin{aligned}\Im(t) &= \sum_{j=A,B} \lambda_1^j(e^{it(\omega_1-\omega_2)}\hat{\sigma}_{12}^j + e^{-it(\omega_1-\omega_2)}\hat{\sigma}_{21}^j)(e^{-i\Omega t}\hat{A} + e^{i\Omega t}\hat{A}^\dagger) \\ &\quad +\lambda_2^j(e^{it(\omega_1-\omega_3)}\hat{\sigma}_{13}^j + e^{-it(\omega_1-\omega_3)}\hat{\sigma}_{31}^j)(e^{-i\Omega t}\hat{A} + e^{i\Omega t}\hat{A}^\dagger), \qquad (9)\\ \Im_{\text{eff}}(t) &= \sum_{j=A,B} \frac{\lambda_1^j}{2\sqrt{\omega\Omega}}(e^{it\Delta_1}\zeta_+\hat{a}\hat{\sigma}_{12}^j + e^{-it\Delta_1}\zeta_+^*\hat{a}^\dagger\hat{\sigma}_{21}^j) + \frac{\lambda_2^j}{2\sqrt{\omega\Omega}}(e^{it\Delta_2}\zeta_+\hat{a}\hat{\sigma}_{13}^j + e^{-it\Delta_2}\zeta_+^*\hat{a}^\dagger\hat{\sigma}_{31}^j).\end{aligned}$$

where the detuning parameters are given by $\Delta_1 = (\omega_1 - \omega_2) - \Omega$ and $\Delta_2 = (\omega_1 - \omega_3) - \Omega$.

To obtain the wave function of the considered system, we solve the time-dependent Schrödinger equation $i\dfrac{\partial}{\partial t}|\psi(t)\rangle = \Im_{\text{eff}}|\psi(t)\rangle$. The wave function at any time t can be written in the form

$$\begin{aligned}|\psi(t)\rangle &= \sum_n c_n\Big[\mathtt{X}_1(n,t)|1,1,n\rangle + \mathtt{X}_2(n+1,t)\big(|1,2,n+1\rangle + |2,1,n+1\rangle\big) \\ &\quad +\mathtt{X}_3(n+1,t)\big(|1,3,n+1\rangle + |3,1,n+1\rangle\big) + \mathtt{X}_4(n+2,t)\big(|2,3,n+2\rangle + |3,2,n+2\rangle\big) \\ &\quad +\mathtt{X}_5(n+2,t)|2,2,n+2\rangle + \mathtt{X}_6(n+2,t)|3,3,n+2\rangle\Big]. \qquad (10)\end{aligned}$$

We assume that the field is initially prepared in the coherent state $|\alpha\rangle$ and the atoms enter the cavity in arbitrary pure atomic states. Hence, the wave function at the initial time is given by

$$|\psi(0)\rangle = \Big[\xi_1|1,1\rangle + \xi_2\big(|1,2\rangle + |2,1\rangle\big) + \xi_3\big(|1,3\rangle + |3,1\rangle\big) + \xi_4\big(|2,3\rangle + |3,2\rangle\big) + \xi_5|2,2\rangle + \xi_6|3,3\rangle\Big]\,|\alpha\rangle, \qquad (11)$$

where $|\alpha\rangle = \sum_n c_n|n\rangle$, $c_n = e^{-\bar{n}/2}\,\frac{\bar{n}^{n/2}}{\sqrt{n!}}$ and ξ_l $(l = 1,\ldots,6)$ are arbitrary complex values that satisfy the normalization condition

$$|\xi_1|^2 + 2\sum_{l=2}^{4}|\xi_l|^2 + |\xi_5|^2 + |\xi_6|^2 = 1. \qquad (12)$$

Substituting Eq. (10) in the Schrödinger equation, we obtain six differential equations

$$\begin{aligned} i\dot{\mathtt{X}}_1 &= 2\psi_{n+1}\mathtt{X}_2e^{i\Delta_1 t} + 2\psi_{n+1}\mathtt{X}_3e^{i\Delta_2 t}, & i\dot{\mathtt{X}}_2 &= \psi_{n+2}\mathtt{X}_5e^{i\Delta_1 t} + \psi_{n+1}^*\mathtt{X}_1e^{-i\Delta_1 t} + \psi_{n+2}\mathtt{X}_4e^{i\Delta_2 t} \\ i\dot{\mathtt{X}}_3 &= \psi_{n+2}\mathtt{X}_4e^{i\Delta_1 t} + \psi_{n+2}\mathtt{X}_6e^{i\Delta_2 t} + \psi_{n+1}^*\mathtt{X}_1e^{-i\Delta_2 t}, & i\dot{\mathtt{X}}_4 &= \psi_{n+2}^*\mathtt{X}_3e^{-i\Delta_1 t} + \psi_{n+2}^*\mathtt{X}_2e^{-i\Delta_2 t}, \\ i\dot{\mathtt{X}}_5 &= 2\psi_{n+2}^*\mathtt{X}_2e^{-i\Delta_1 t}, & i\dot{\mathtt{X}}_6 &= 2\psi_{n+2}^*\mathtt{X}_3e^{-i\Delta_2 t}, \end{aligned} \qquad (13)$$

where $\psi_n = \lambda\sqrt{n}\zeta_+/2\sqrt{\omega\Omega}$, such that $\omega^2 \gg \gamma^2$, $\lambda_1^j = \lambda_2^j = \lambda$, and $\Omega \simeq \omega - \gamma^2/2\omega$. It is obvious that the coefficients of this coupled system of differential equations are time-dependent ones. We can avoid this problem using the transforms

$$\begin{aligned} \mathtt{X}_1(n,t) &= \bar{\mathtt{X}}_1(n,t)e^{\frac{i}{2}(\Delta_1+\Delta_2)t}, & \mathtt{X}_2(n+1,t) &= \bar{\mathtt{X}}_2(n+1,t)e^{\frac{i}{2}(\Delta_2-\Delta_1)t}, \\ \mathtt{X}_3(n+1,t) &= \bar{\mathtt{X}}_3(n+1,t)e^{\frac{i}{2}(\Delta_1-\Delta_2)t}, & \mathtt{X}_4(n+2,t) &= \bar{\mathtt{X}}_4(n+2,t)e^{\frac{-i}{2}(\Delta_1+\Delta_2)t}, \\ \mathtt{X}_5(n+2,t) &= \bar{\mathtt{X}}_5(n+2,t)e^{\frac{i}{2}(\Delta_2-3\Delta_1)t}, & \mathtt{X}_6(n+2,t) &= \bar{\mathtt{X}}_6(n+2,t)e^{\frac{i}{2}(\Delta_1-3\Delta_2)t}, \end{aligned} \qquad (14)$$

and the Laplace transform to arrive at

$$\begin{pmatrix} s+i\Delta_{12} & 2i\psi_{n+1} & 2i\psi_{n+1} & 0 & 0 & 0 \\ i\psi^*_{n+1} & s+i\Delta_{21} & 0 & i\psi_{n+2} & i\psi_{n+2} & 0 \\ i\psi^*_{n+1} & 0 & s+i\bar{\Delta}_{12} & i\psi_{n+2} & 0 & i\psi_{n+2} \\ 0 & i\psi^*_{n+2} & i\psi^*_{n+2} & s-i\Delta_{12} & 0 & 0 \\ 0 & 2i\psi^*_{n+2} & 0 & 0 & s+i\tilde{\Delta}_{21} & 0 \\ 0 & 0 & 2i\psi^*_{n+2} & 0 & 0 & s+i\tilde{\Delta}_{12} \end{pmatrix} \begin{pmatrix} L(\bar{\mathtt{X}}_1) \\ L(\bar{\mathtt{X}}_2) \\ L(\bar{\mathtt{X}}_3) \\ L(\bar{\mathtt{X}}_4) \\ L(\bar{\mathtt{X}}_5) \\ L(\bar{\mathtt{X}}_6) \end{pmatrix} = \begin{pmatrix} \bar{\mathtt{X}}_1(0) \\ \bar{\mathtt{X}}_2(0) \\ \bar{\mathtt{X}}_3(0) \\ \bar{\mathtt{X}}_4(0) \\ \bar{\mathtt{X}}_5(0) \\ \bar{\mathtt{X}}_6(0) \end{pmatrix}, \quad (15)$$

where

$$\begin{aligned} &\Delta_{12} = (\Delta_1 + \Delta_2)/2, \quad \bar{\Delta}_{12} = (\Delta_1 - \Delta_2)/2, \quad \tilde{\Delta}_{12} = (\Delta_1 - 3\Delta_2)/2, \\ &\Delta_{21} = (\Delta_2 - \Delta_1)/2, \quad \tilde{\Delta}_{21} = (\Delta_2 - 3\Delta_1)/2. \end{aligned} \quad (16)$$

After some straightforward calculations, we obtain the solution of Eq. (15) using the initial state, Eq. (11). Here, we reveal the complete solution for $\mathtt{X}_1(n,t)$,

$$\mathtt{X}_1(n,t) = \sum_{e=1}^{6} \alpha_e e^{(s_e + i\Delta_{12})t}, \qquad \alpha_e = \frac{F_1(s_e)}{\Omega_e}, \quad (17)$$

where

$$\Omega_e = \prod_{d=1,\ldots,6}^{e\neq d} (s_e - s_d), \qquad F_1(s) = \bar{\mathtt{X}}_1(0)a_1(s) - 2\,i\,\psi_{n+1}a_2(s) + 2\,i\,\psi_{n+1}a_3(s). \quad (18)$$

The solutions of $\mathtt{X}_2(n+1,t)$, $\mathtt{X}_3(n+1)$, $\mathtt{X}_4(n+2)$, $\mathtt{X}_5(n+2)$, and $\mathtt{X}_6(n+2)$ can be obtained in the same way. We have

$$a_1(s) = \begin{vmatrix} s+i\Delta_{21} & 0 & i\psi_{n+2} & i\psi_{n+2} & 0 \\ 0 & s+i\bar{\Delta}_{12} & i\psi_{n+2} & 0 & i\psi_{n+2} \\ i\psi^*_{n+2} & i\psi^*_{n+2} & s-i\Delta_{12} & 0 & 0 \\ 2i\psi^*_{n+2} & 0 & 0 & s+i\tilde{\Delta}_{21} & 0 \\ 0 & 2i\psi^*_{n+2} & 0 & 0 & s+i\tilde{\Delta}_{12} \end{vmatrix},$$

$$a_2(s) = \begin{vmatrix} \bar{\mathtt{X}}_2(0) & 0 & i\psi_{n+2} & i\psi_{n+2} & 0 \\ \bar{\mathtt{X}}_3(0) & s+i\bar{\Delta}_{12} & i\psi_{n+2} & 0 & i\psi_{n+2} \\ \bar{\mathtt{X}}_4(0) & i\psi^*_{n+2} & s-i\Delta_{12} & 0 & 0 \\ \bar{\mathtt{X}}_5(0) & 0 & 0 & s+i\tilde{\Delta}_{21} & 0 \\ \bar{\mathtt{X}}_6(0) & 2i\psi^*_{n+2} & 0 & 0 & s+i\tilde{\Delta}_{12} \end{vmatrix}, \quad (19)$$

$$a_3(s) = \begin{vmatrix} \bar{\mathtt{X}}_2(0) & s+i\Delta_{21} & i\psi_{n+2} & i\psi_{n+2} & 0 \\ \bar{\mathtt{X}}_3(0) & 0 & i\psi_{n+2} & 0 & i\psi_{n+2} \\ \bar{\mathtt{X}}_4(0) & i\psi^*_{n+2} & s-i\Delta_{12} & 0 & 0 \\ \bar{\mathtt{X}}_5(0) & 2i\psi^*_{n+2} & 0 & s+i\tilde{\Delta}_{21} & 0 \\ \bar{\mathtt{X}}_6(0) & 0 & 0 & 0 & s+i\tilde{\Delta}_{12} \end{vmatrix},$$

and s_e, $e = 1, \ldots, 6$, are the roots of the equation

$$\mu_0 + \mu_1 s + \mu_2 s^2 + \mu_3 s^3 + \mu_4 s^4 + \mu_5 s^5 + s^6 = 0, \tag{20}$$

where

$$\begin{aligned}
\mu_0 &= \frac{(\Delta_1+\Delta_2)^2}{64}\big[(\Delta_1-3\Delta_2)(\Delta_1-\Delta_2)^2(3\Delta_1-\Delta_2) - 32|\psi_{n+2}|^2\left(4|\psi_{n+1}|^2 - 4|\psi_{n+2}|^2 + (\Delta_1-\Delta_2)^2\right)\big],\\
\mu_1 &= -\frac{i(\Delta_1+\Delta_2)}{16}\big[-4\left(\Delta_1^2 - 14\Delta_1\Delta_2 + \Delta_2^2\right)|\psi_{n+2}|^2 + 8|\psi_{n+1}|^2\left(16|\psi_{n+2}|^2 + (3\Delta_1-\Delta_2)(\Delta_1-3\Delta_2)\right)\\
&\quad + \left(\Delta_1^2-\Delta_2^2\right)^2\big],\\
\mu_2 &= |\psi_{n+1}|^2\left(8|\psi_{n+2}|^2 + \Delta_1^2 - 14\Delta_1\Delta_2 + \Delta_2^2\right) + \frac{3}{2}(\Delta_1+\Delta_2)^2|\psi_{n+2}|^2 + 8|\psi_{n+2}|^4\\
&\quad + \frac{1}{16}(7\Delta_1^4 - 20\Delta_1^3\Delta_2 + 10\Delta_1^2\Delta_2^2 - 20\Delta_1\Delta_2^3 + 7\Delta_2^4),\\
\mu_3 &= -\frac{1}{2}i(\Delta_1+\Delta_2)\left(12|\psi_{n+1}|^2 + 6|\psi_{n+2}|^2 + \Delta_1^2 + \Delta_2^2\right),\\
\mu_4 &= 4|\psi_{n+1}|^2 + 6|\psi_{n+2}|^2 + \frac{5}{4}(\Delta_1-\Delta_2)^2, \qquad \mu_5 = -i(\Delta_1+\Delta_2).
\end{aligned} \tag{21}$$

3. Physical Properties

After obtaining the final form of the wave function, Eq. (10), we next study the various physical properties of the system and the effects of the initial atomic states and damping parameter have on these physical properties. Note that in all situations, we set $\delta_1 = \delta_2 = \lambda$, such that $\delta_1 = (\omega_1 - \omega_2) - \omega$, $\delta_2 = (\omega_1 - \omega_3) - \omega$, and $\lambda = 0.01\,\omega$.

3.1. Degree of Entanglement

To evaluate the DEM between the field and the atoms, we use the linear entropy measure, which is defined as [36]

$$\mathtt{S} = 1 - \mathrm{Tr}(\varrho_{\mathtt{AB}}^2), \tag{22}$$

where

$$\varrho_{\mathtt{AB}} = \mathrm{Tr}_{\mathtt{f}}(|\psi(t)\rangle\langle\psi(t)|), \tag{23}$$

with the atomic basis $\{|1,1\rangle, |1,2\rangle, |1,3\rangle, |2,1\rangle, |2,2\rangle, |2,3\rangle, |3,1\rangle, |3,2\rangle, |3,3\rangle\}$, the diagonal matrix elements given by

$$\varrho_{11} = \sum_{n=0}^{\infty}|c_n|^2|\mathtt{X}_1(n,t)|^2, \qquad \varrho_{ii} = \sum_{n=0}^{\infty}|c_n|^2|\mathtt{X}_j(n+1,t)|^2, \qquad \varrho_{jj} = \sum_{n=0}^{\infty}|c_n|^2|\mathtt{X}_j(n+2,t)|^2, \tag{24}$$

and the off-diagonal matrix elements given by

$$\begin{aligned}
\varrho_{1i} &= \sum_{n=0}^{\infty} c_{n+1}c_n^*\mathtt{X}_1(n+1,t)\mathtt{X}_i(n+1,t)^*, & \varrho_{1j} &= \sum_{n=0}^{\infty} c_{n+2}c_n^*\mathtt{X}_1(n+2,t)\mathtt{X}_j(n+2,t)^*,\\
\varrho_{23} &= \sum_{n=0}^{\infty} |c_n|^2\mathtt{X}_2(n+1,t)\mathtt{X}_3(n+1,t)^*, & \varrho_{2j} &= \sum_{n=0}^{\infty} c_{n+1}c_n^*\mathtt{X}_2(n+2,t)\mathtt{X}_j(n+2,t)^*,\\
\varrho_{3j} &= \sum_{n=0}^{\infty} c_{n+1}c_n^*\mathtt{X}_3(n+2,t)\mathtt{X}_j(n+2,t)^*, & \varrho_{45} &= \sum_{n=0}^{\infty} |c_n|^2\mathtt{X}_4(n+2,t)\mathtt{X}_5(n+2,t)^*, \qquad (25)\\
\varrho_{46} &= \sum_{n=0}^{\infty} |c_n|^2\mathtt{X}_4(n+2,t)\mathtt{X}_6(n+2,t)^*, & \varrho_{56} &= \sum_{n=0}^{\infty} |c_n|^2\mathtt{X}_5(n+2,t)\mathtt{X}_6(n+2,t)^*,\\
\varrho_{i1} &= \varrho_{1i}^*, & \varrho_{j1} &= \varrho_{1j}^*, \qquad (i=2,3, j=4,5,6).
\end{aligned}$$

To show the influence of damping on the linear entropy of this system, we plotted the time evolution of the linear entropy (Fig. 2) when the field is initially in the coherent state with the mean photon number $\bar{n} = 25$. However, for undamped instances, $\eta = 0.0$, and various initial atomic states a_1, b_1, c_1 in Fig. 2,

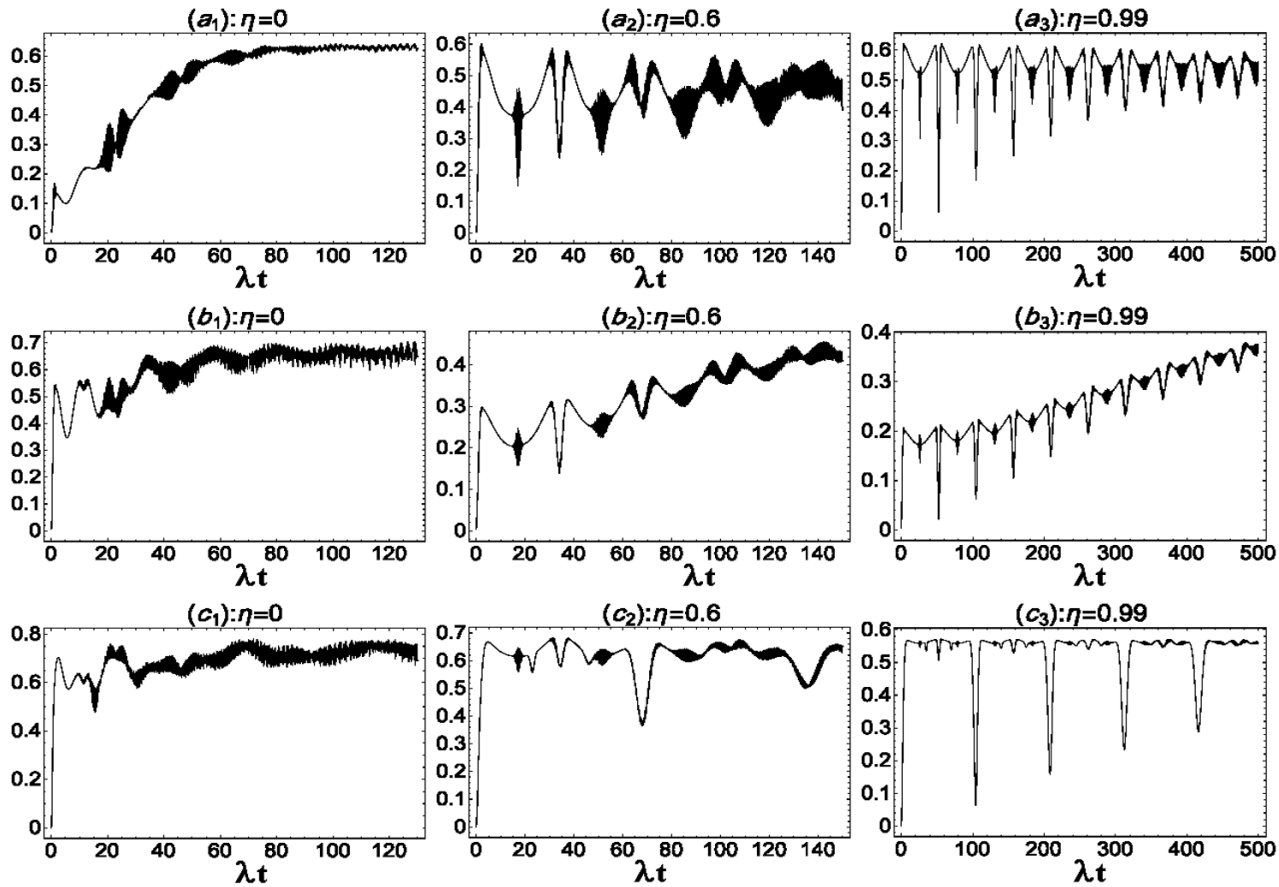

Fig. 2. Linear entropy versus scaled time λt with $\bar{n} = 25$, $\delta_1 = \delta_2 = \lambda$, and $\lambda/\omega = 0.01$ for different damping parameter values η. For the initial atomic state in (a_1, a_2, a_3) $\xi_i = 1/3$, $i = 1, 2, 3, 4, 5, 6$, in (b_1, b_2, b_3) $\xi_i = 1/\sqrt{6}$, $i = 2, 3, 4$, and in (c_1, c_2, c_3) $\xi_2 = 1/\sqrt{2}$.

such that the two atoms are initially in a superposition of all states $\xi_l = 1/3$, $l = (1, 2, 3, 4, 5, 6)$ and $\xi_l = 1/\sqrt{6}$, $l = (2, 3, 4)$, and $\xi_2 = 1/\sqrt{2}$, we see that after a short time the entropy rapidly oscillates around its upper value (nearly 0.65). Hence, there is an increase in the maximum DEM between the two atoms and the field. Note that the heights of the revivals in probability are very small, and the value of the probability almost remains at a constant value of 0.7; see a_1, b_1, c_1 in Fig. 2. However, the DEM has increased and it reaches its maximum during collapse. In what follows, we use linear entropy to discuss the DEM for different values of the damped parameters and various initial atomic states. For $\eta = 0.6$, the temporal behavior of the linear entropy is plotted in Fig. 2 as a_2, b_2, c_2.

In a_3, b_3, c_3 in Fig. 2, we note that there is an increase in the reduction of the maximum DEM between the two atoms and the field, which nearly reaches (0.6, 0.63, 0.55) for the initial states in a superposition of all states $\xi_l = 1/3$, $\xi_l = 1/\sqrt{6}$, and $\xi_2 = 1/\sqrt{2}$, respectively. A comparison between a_1, b_1, c_1, a_2, b_2, c_2, and a_3, b_3, c_3 in Fig. 2 shows that the temporal behavior of the linear entropy is very sensitive to the damping parameters.

3.2. Mandel $\mathbf{Q_m}$ Parameter

The Mandel Q_m parameter is a very useful quantity for the investigation of quantum statistical properties of any state. It is defined as [37]

$$Q_m = \frac{\langle (a^\dagger a)^2 \rangle - \langle a^\dagger a \rangle^2 - \langle a^\dagger a \rangle}{\langle a^\dagger a \rangle}\,; \tag{26}$$

negative values of Q_m correspond to sub-Poissonian statistics, indicating nonclassicality of the given state.

We plotted the time behavior of Q_m against the scaled time λt (Fig. 3). The initial field is the coherent state, with $\bar{n} = 25$. However, a different value for the damping parameter is chosen with various initial atomic states. For $\eta = 0$ (no damping), the oscillations tend to rise to positive regions more often than when damping is present. Furthermore, we note that revivals and collapses are clearly evident and is a distinctive quantum behavior of the state in Fig. 3 (a_1, b_1, c_1). We examined the effects of damping on the temporal evolution of the Mandel Q_m parameter in Fig. 3 (a_2, b_2, c_2). For $\eta = 0.6$, the Mandel Q_m parameter varies between positive and negative values, which means that the photons display super- or sub-Poissonian statistics at different intervals of time; a long collapse-revival phenomenon is clearly seen for all instances. We note that in Fig. 3 (a_3, b_3, c_3), the depth of negativity has increased. Also, we observe that the Mandel parameter descends towards the negative region and becomes negative, indicating full sub-Poissonian statistics of the field at all times, and the super-Poissonian statistics part of the field disappears. Clearly, when the two atoms are prepared initially in a separable atomic state, the effect of damping is stronger, making the Q_m curves go negative and indicating nonclassical features.

3.3. Normal Squeezing

To discuss the normal squeezing of the field, we introduce two quadrature field operators $\hat{x} = \dfrac{a + a^\dagger}{\sqrt{2}}$ and $\hat{p} = \dfrac{a + a^\dagger}{\sqrt{2}i}$, the variances of position $(\Delta x)^2$ and momentum $(\Delta p)^2$, and the squeezing of x and p, which is expressed by $S_l = 2(\Delta l)^2 - 1$ with $l = x, p$. Subsequently, a state is squeezed in the l direction

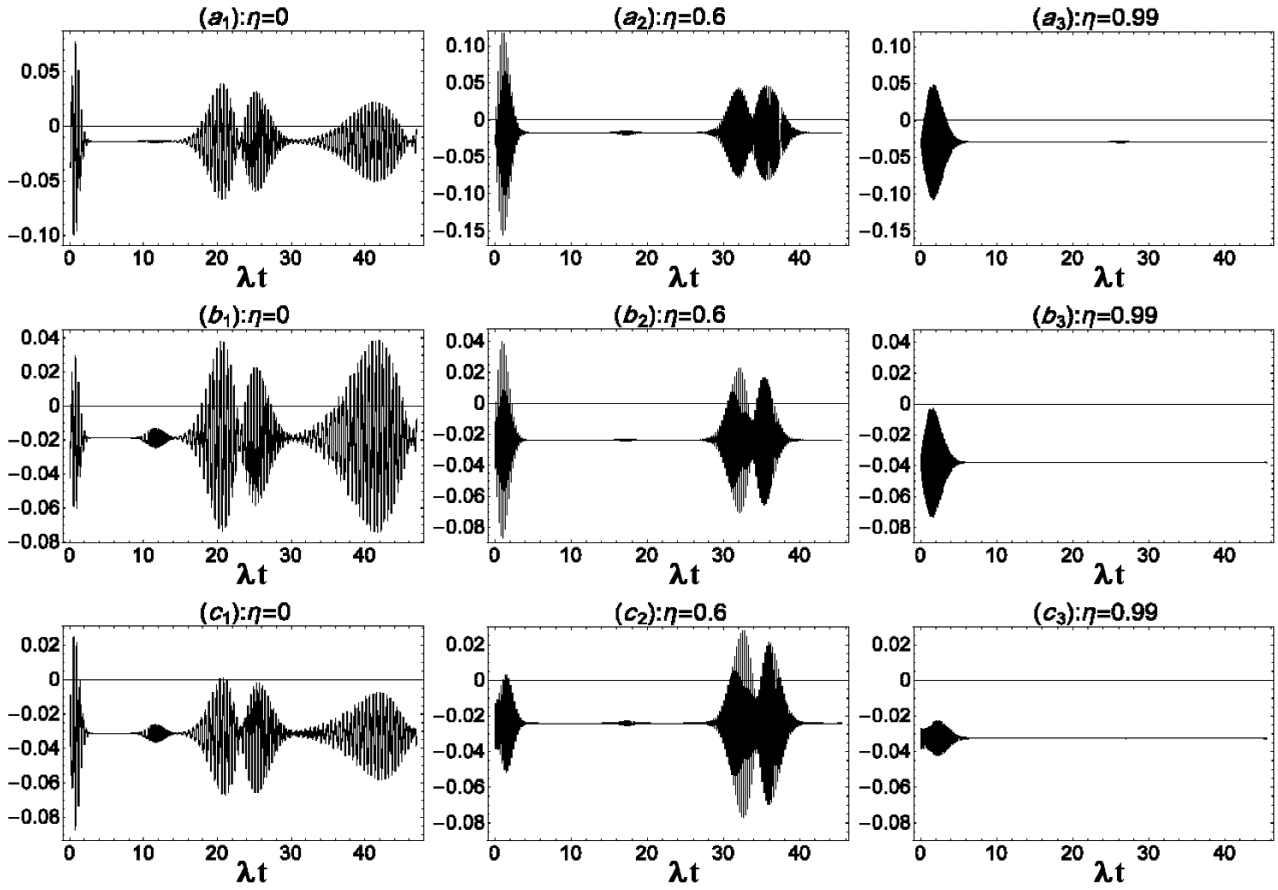

Fig. 3. Mandel Q_m parameter versus scaled time λt, with $\bar{n} = 25$, $\delta_1 = \delta_2 = \lambda$, and $\lambda/\omega = 0.01$, for different values of the damping parameter η. All initial atomic states are as stated in Fig. 2.

if the inequality $-1 < S_l < 0$ holds. These parameters can be rewritten as

$$S_x = 2\langle \hat{a}^\dagger \hat{a}\rangle + 2\,\mathrm{Re}\langle \hat{a}^{\dagger 2}\rangle - 4(\mathrm{Re}\langle \hat{a}^\dagger\rangle)^2, \qquad S_p = 2\langle \hat{a}^\dagger \hat{a}\rangle - 2\,\mathrm{Re}\langle \hat{a}^{\dagger 2}\rangle - 4(\mathrm{Re}\langle \hat{a}^\dagger\rangle)^2. \tag{27}$$

The time evolution of the normal squeezing parameter corresponding to a fixed position is plotted with the same data as in Fig. 2 for no damping, $\eta = 0.0$. We find that, for all instances, squeezing exists at position x. In Fig. 4 (a_1, b_1, c_1), the curves for squeezing lie in the positive region, ensuring that, apart from a short initial period, the introduced field is not squeezed with the initial atomic state. In Fig. 4 (a_2, b_2, c_2) with increased damping $\eta = 0.6$, the strength of normal squeezing can be observed for all initial states $\xi_l = 1/3$, $l = (1, 2, 3, 4, 5, 6)$ as in Fig. 4 (a_2) and $\xi_l = 1/\sqrt{6}$, $l = (2, 3, 4)$ as in Fig. 4 (b_2), while weakness of normal squeezing was observed for the initial state $\xi_2 = 1/\sqrt{2}$ as in Fig. 4 (c_2). However, in Fig. 4 (a_3, b_3, c_3), the evaluated normal squeezing occurs in some finite intervals of time, while with increased damping $\eta = 0.99$, the strength of normal squeezing occurs more clearly. Furthermore, a comparison between Fig. 4 (a_1) and (a_2, a_3), Fig. 4 (b_1) and (b_2, b_3), and Fig. 4 (c_1) and (c_2, c_3), for the different initial atomic states, shows that by increasing η the intervals of this nonclassical effect in x are augmented. Also, our results suggest that squeezing in the x component in the initial atomic state $\xi_2 = 1/\sqrt{2}$ is weaker than for the other two instances.

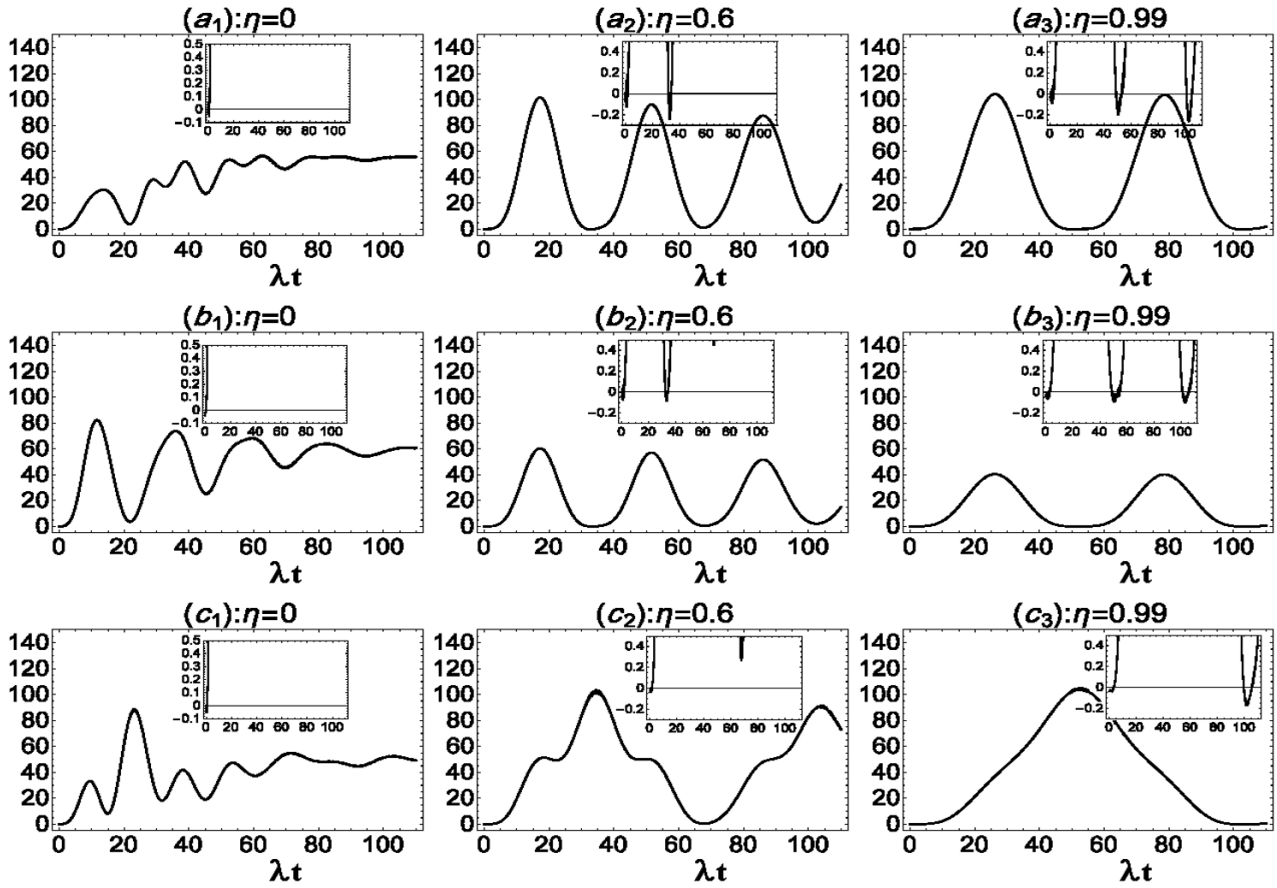

Fig. 4. Normal squeezing parameter S_x plotted as a function of scaled time λt, with $\bar{n} = 25$, $\delta_1 = \delta_2 = \lambda$, and $\lambda/\omega = 0.01$, for different values of the damping parameter η. All initial atomic states are as stated in Fig. 2.

4. Summary

From an analysis of damping based on the CK Hamiltonian, we investigated a few nonclassical features such as quantum entanglement for two Λ-type three-level atoms, initially prepared in different initial atomic states, and a single-mode field. Also we evaluated the Mandel parameter as well as quadrature squeezing. The results for the effect of damping and the initial atomic states on these features showed that the state of the system plays an important role in the time evolution of entanglement. We conclude by listing the main results:

1. In the absence of damping, the maximum DEM value (∼0.77) takes place when the two atoms are initially in $\xi_2(|1,2\rangle + |2,1\rangle)$, $\xi_2 = 1/\sqrt{2}$. In contrast, when damping is present, the maximum DEM value decreases but gradually increases with time.

2. In the absence of damping, the Mandel parameter becomes more negative when the two atoms are initially in $\xi_2(|1,2\rangle + |2,1\rangle)$, $\xi_2 = 1/\sqrt{2}$. Furthermore, when damping is present, the revival periods decrease and fluctuate below zero with increasing damping.

3. In the absence of damping, normal squeezing of the x component in the initial atomic state $\xi_2(|1,2\rangle +$

$|2,1\rangle$), $\xi_2 = 1/\sqrt{2}$ is weaker than for the other two instance. Squeezing becomes stronger with increase in damping.

Acknowledgments

We thank Richard Haase, PhD, from Edanz Group (www.edanzediting.com/ac) for editing a draft of this manuscript.

References

1. E. T. Jaynes and F. W. Cummings, *Proc. IEEE*, **51**, 89 (1963).
2. G. Rempe, H. Walther, and N. Klein, *Phys. Rev. Lett.*, **58**, 353 (1987).
3. B. W. Shore and P. L. Knight, *J. Mod. Opt.*, **40**, 1195 (1993).
4. V. I. Man'ko and S. S. Safonov, *Teor. Mat. Fiz.*, **112**, 467 (1997).
5. V. V. Dodonov and V. I. Man'ko, *Phys. Rev. A*, **20**, 550 (1979).
6. O. V. Man'ko, *J. Russ. Laser Res.*, **17**, 439 (1996).
7. V. I. Man'ko, *J. Russ. Laser Res.*, **17**, 579 (1996).
8. A.-S. F. Obada, M. M. A. Obada, E. M. Obada, and S. I. Ali, *Opt. Commun.*, **287**, 215 (2013).
9. F. Yadollahi and M. K. Yadollahi, *Opt. Commun.*, **284**, 608 (2011).
10. M. K. Tavassoly and F. Yadollahi, *Int. J. Mod. Phys. B*, **26**, 1250027 (2012).
11. M. Sahrai and H. Tajalli, *J. Opt. Soc. Am. B.*, **30**, 512 (2013).
12. H. R. Baghshahi and M. K. Tavassoly, *Phys. Scr.*, **89**, 075101 (2014).
13. V. Buzek, *Phys. Rev. A.*, **39**, 3196 (1989).
14. J. M. Fink, M. Fink, M. Fink, et al., *Nature*, **454**, 315 (2008).
15. A. Joshi, *Phys. Rev. A.*, **62**, 043812 (2000).
16. E. K. Bashkirov and M. S. Rusakova, *Opt. Commun.*, **281**, 4380 (2008).
17. E. Faraj, M. K. Tavassoly, and H. R. Tavassoly, *Int. J. Theor. Phys.*, **55**, 2573 (2016).
18. H. R. Baghshahi, M. K. Tavassoly, and S. J. Tavassoly, *Quantum Inform. Process.*, **14**, 1279 (2015).
19. D. Tavassoly and M. D. Tavassoly, *Quantum Processes, Systems, and Information*, Cambridge University Press, New York (2010).
20. J. R. Choi, S. Lakehal, M. Lakehal, and S. Lakehal, *Electromagn. Res. Lett. Prog.*, **44**, 71 (2014).
21. I. Lakehal and A. Pinheiro, *Theor. Phys. Prog.*, **125**, 1133 (2011).
22. J. R. Choi, *Int. J. Theor. Phys.*, **45**, 176 (2006).
23. J. R. Choi, *Pramana.*, **62**, 13 (2004).
24. S. P. J. Choi, *Phys. A: Math. Gen.*, **36**, 12089 (2003).
25. U. Weiss, *Quantum Dissipative Systems*, World Scientific, Singapore (1999).
26. M. Razavy, *Classical and Quantum Dissipative Systems*, World Scientific, Singapore (2005).
27. E. Kanai, *Theor. Phys. Prog.*, **3**, 440 (1948).
28. P. Caldirola, *Nuovo Cimento*, **18**, 393 (1941).
29. H. Goldstein, *Classical Mechanics*, Addison-Wesley, New York (1965).
30. M. S. Abdalla, *Phys. Rev. A*, **33**, 2870 (1986).
31. J. Aliaga, G. Crespo, and A. N. Crespo, *Phys. Rev. A*, **42**, 4325 (1990).
32. M. S. Abdalla, *Phys. Rev. A.*, **170**, 393 (1991).
33. R. Abdalla and M. K. Tavassoly, *Int. J. Theor. Phys.*, **65**, 1218 (2017).
34. M. O. Scully and M. S. Zubairy, *Quantum Optics*, Cambridge University Press, New York (1997).
35. R. Daneshmand and M. K. Tavassoly, *Laser Phys.*, **26**, 065204 (2016).
36. J. I. Kim, M. C. Kim, and A. F. R. de Toledo Piza, *Quantum Inform. Process.*, **77**, 207 (1996).
37. L. Mandel, *J. Russ. Laser Res.*, **4**, 205 (1979).